ADVANCED FUNCTIONAL MATERIALS
www.afm-journal.de

Photochemical Transformation of Fullerenes

*Jia Wang, Jenny Enevold, and Ludvig Edman**

Experimental findings and associated theoretical insights regarding the photochemical transformation of fullerenes are reported, which challenge the conventional wisdom in the field and point out a viable path towards improved fullerene-based electronic devices. It is shown that the efficiency of the photochemical monomer-to-dimer transformation of the fullerene [6,6′]-phenyl-C_{61}-butyric acid methyl ester (PCBM) is strongly dependent on the light intensity, and this is utilized to demonstrate that direct patterning of an electroactive PCBM film can be effectuated by sub-second UV-light exposure followed by development in a tuned developer solution. By straightforward analytical reasoning, it is demonstrated that the observed intensity-dependent monomer-to-dimer transformation dictates that a significant back-reaction to the ground state must be in effect, which presumably originates from the excited-triplet state. By a combination of numerical modeling and analytical argumentation, it is further shown that the final dimer formation must constitute a bi-excited reaction between two neighboring monomers photo-excited to the triplet state.

1. Introduction

Fullerenes are nanometer-sized spherical-shaped molecules, comprising a shell of carbon atoms intra-molecularly bonded via a combination of single and double bonds.[1,2] This novel group of nanomaterials exhibit a wide range of exotic and appealing properties, which render them interesting study objects for fundamental investigations[3–9] as well as exploitable as active materials in a plethora of ubiquitous applications, notably photovoltaic devices,[10–17] transistor arrays,[18–20] and integrated circuits.[21–24]

One interesting property of fullerene molecules (monomers) is that they can be transformed into dimeric or polymeric structures under illumination by UV and visible light, where the chemical coupling between different fullerene monomers is effectuated by a photo-induced break-up of intra-molecular double bonds.[25] As this photochemical transformation is accompanied by a distinctly lowered solubility in hydrophobic solvents, it is possible to utilize fullerenes as a sacrificial photoresist material for the lithographic creation of two-dimensional structures in various thin films.[26,27] Moreover, as it has recently been demonstrated that the patterned fullerene film can retain its electronic activity, a straightforward and material-conservative path towards patterned electronic circuits is viable, where the fullerene film functions as both (negative) photo-resist and electronic material.[28–30] Interestingly, it has been shown that an area-selective removal of the fullerene component in fullerene-conjugated polymer blend films can be executed with the same two-step approach,[23] and this opportunity has been utilized for the realization of complementary transistor circuits, such as inverters[23]and oscillators,[21] from a single-layer film.

Here, we report on experimental and theoretical findings regarding the photo-induced monomer-to-dimer transformation of fullerenes, which challenge the current conventional wisdom in the field. We find that the efficiency of dimerization of the commonly employed fullerene [6,6′]-phenyl-C_{61}-butyric acid methyl ester (PCBM) is *positively* influenced by an increasing intensity of the incident UV light. This experimental observation provides a straightforward guideline towards an improved patterning-process throughput, but also dictates that a significant back-reaction to the PCBM ground state must be in effect in parallel with the forward monomer-to-dimer transformation. We further demonstrate that the final PCBM dimer-formation reaction is of a bi-excited nature, as it is effectuated between two neighboring PCBM molecules, both being in a photo-excited triplet state.

2. Results and Discussion

The two-step patterning method of fullerene films for electronic applications comprises an initial selective-area light exposure and a subsequent solution development, as schematically depicted in **Figure 1**a. During the first step, the fullerene film is conveniently selectively exposed to UV-visible light via the use of a shadow mask. The light exposure triggers a photochemical reaction between exposed fullerene molecules, so that the exposed parts of the film transform into a dimerized/polymerized state, with a concomitant notably decreased solubility. During the second step, the film is developed via complete immersion into a tuned developer solution, which selectively removes the non-exposed, high-solubility fullerene monomers while leaving the exposed regions intact. The outcome of the process, as appropriately executed, is thus that the "insoluble" dimerized/polymerized fullerenes remain and form a negative pattern on the substrate where the exposure light was incident.

Dr. J. Wang, J. Enevold, Prof. L. Edman
The Organic Photonics and Electronics Group
Department of Physics
Umeå University
SE-901 87 Umeå, Sweden
E-mail: ludvig.edman@physics.umu.se

DOI: 10.1002/adfm.201203386

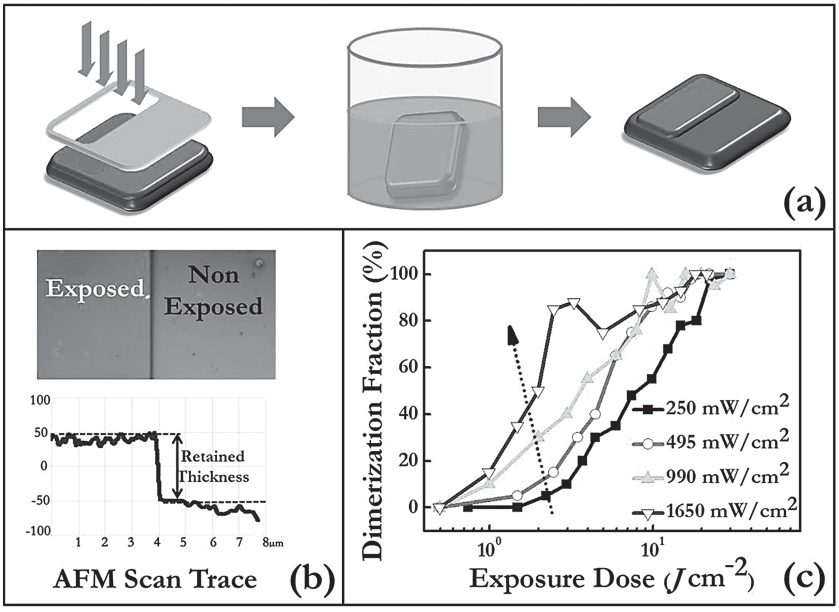

Figure 1. a) Schematic presenting the two-step patterning process of fullerene films, comprising selective-area light exposure and solution development. b) Top: A (1.4 mm × 2 mm) photograph of a patterned PCBM film on a SiO_2/Si substrate, depicting retained (blue-green) PCBM in the left region and a (brown) bare SiO_2 substrate surface in the right region. Bottom: An AFM scan trace measuring the retained PCBM thickness after a two-step patterning experiment. c) Measured dimerization fraction as a function of UV-light exposure dose. The different curves represent different UV-light intensities, with the arrow indicating an increase in light intensity.

A representative result of the two-step patterning process is visualized in the photograph in the upper part of Figure 1b, where the left (blue-green) area of a 100-nm-thick PCBM film was selectively exposed to UV-light (λ_{peak} = 365 nm) during the initial exposure step, and the right non-exposed area of the same film accordingly was removed during the subsequent development step, being immersion into a developer solution (acetone: chloroform = 7: 1 by volume). We mention that we selected UV light over visible light for the exposure step, as the higher absorption of PCBM in the UV-wavelength range, as compared to the visible-wavelength range, correlates to a more efficient exposure step, i.e., a more efficient monomer-to-dimer transformation.[30]

It is notable that the UV-light intensity and the exposure time in the experiment presented in Figure 1b were selected so that a complete dimerization was attained in the exposed PCBM region, but that a lower UV-light intensity and/or a shorter exposure time can induce partial PCBM dimerization instead. In the latter scenario, the non-dimerized PCBM molecules in the exposed regions will also be removed by the developer solution, and a quantitative measure of the dimerization fraction in the exposed regions is available as the quotient between the thickness of the pristine PCBM film and the thickness of the exposed-and-developed PCBM film, as extracted from AFM measurements. An example of an AFM measurement of the thickness of an exposed-and-developed film is presented in the lower part of Figure 1b.

Figure 1c presents experimental results on the dimerization fraction in a PCBM film as a function of exposure dose, recorded at four different UV-light intensities (the dotted arrow indicates increasing intensity). The exposure dose is calculated as the UV-light intensity multiplied by the exposure time, and both properties could be controlled with high accuracy, as described in section I of the Supporting Information. Importantly, the experimental data unambiguously demonstrate that the efficiency of the PCBM dimerization process increases with increasing light intensity. In other words, fewer photons are required to induce a PCBM dimerization reaction at a higher photon flux. Apart from the interesting intellectual challenge this observation poses (which will be addressed below), we note that it also points out a practical path towards more energy- and time-efficient patterning of fullerene-based transistor arrays and logical circuits via the use of higher-intensity light. In this context, we mention that it is, for instance, possible to fully photo-transform a 100-nm-thick PCBM film in a mere 1.0 s by exposing it to UV-light with an intensity of 8000 mW/cm^2.

It is noteworthy that our observation of an intensity-dependent exposure dose is in conflict with the conclusion drawn by P.C. Eklund and co-workers in a pioneering study on the photo-induced dimerization of C_{60} fullerene thin films.[31,32] The generic reaction scheme preceding fullerene dimerization is presented in **Figure 2**a, where k_1–k_6 represents the rate constants of the possible reaction paths between the ground-state monomer, M, the singlet-excited monomer, $^1M^*$, the triplet-excited monomer, $^3M^*$, and the dimer, D. Note that monomers in the higher excited singlet states are omitted from the diagram, as they decay very rapidly down to the first excited singlet state;[33–35] this rationalizes why the symbol $^1M^*$ is used collectively for the end state of the first excitation step. The division into a k_5 and k'_5 path describes two alternative reaction paths to the D state, and will be discussed in detail later.

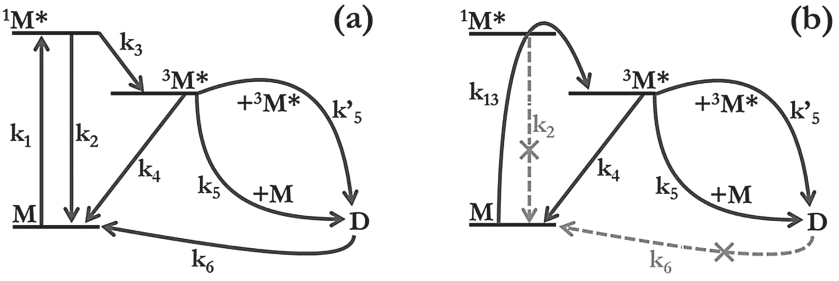

Figure 2. a) Generic energy-level diagram with associated rate constants, k_i, for a fullerene monomer during a dimerization process, with D representing the dimer state. b) Simplified energy-level diagram, as employed in the theoretical treatment, with the zero rate constants crossed out.

Eklund et al. interpreted their experimental Raman spectroscopy data as though the overall M → D reaction-rate constant was limited by, and proportional to, the incident light intensity, and therefore suggested that only a single photon is required to be absorbed in order for a dimer to form.[32,36] Notably, all back-reaction paths, i.e., k_2, k_4 and k_6, must in such a scenario be effectively zero. As a unity absorbed-photon-to-dimer yield is in obvious contradiction to our finding of an intensity-dependent dimerization efficiency (see Figure 1c and accompanying discussion), we set out to analyze our data in more detail; specifically, we are interested in calculating our attained absorbed-photon-to-dimer efficiency.

The number of dimers per unit area in a completely dimerized PCBM film is given by

$$N_{\mathrm{dim}} = \frac{\rho d N_{\mathrm{A}}}{2 M_{\mathrm{w}}}, \tag{1}$$

where ρ is the material density (1.5 g·cm^{-3}),[37] d is the pristine PCBM film thickness (100 nm), N_{A} is Avogadro's number, and M_{w} is the molecular weight of a PCBM monomer (910.88 g·mol^{-1}).

The number of photons absorbed by ground-state monomers per unit area can be calculated from

$$N_{\mathrm{abs}}(T) = I\frac{\lambda}{hc}\int_0^T \left(1 - e^{-\alpha d_{\mathrm{M}}(t)}\right)dt \tag{2}$$

where I is the light intensity, λ is the wavelength of the exposure light (set to λ_{peak} = 365 nm), h is Planck's constant, c is the speed of light, α is the absorption coefficient (1.13 · 10^{-5} cm^{-1}),[30] and $d_{\mathrm{M}}(t)$ is the thickness of *ground-state* monomers. A challenge is that $d_{\mathrm{M}}(t)$ changes during an exposure experiment, as ground-state monomers are transformed into dimers (and singlet- and triplet-excited monomers). However, we have measured α to be essentially the same for PCBM films during different stages of dimerization, which makes it possible to account for the decreasing number of absorbing ground-state monomers during an exposure experiment, by defining an effective ground-state monomer thickness

$$d_{\mathrm{M}}(t) = \mathrm{M}(t)d, \tag{3}$$

where M(t) represents the mass fraction of ground-state monomers in the film at time t. M(t) is accordingly equal to one at the onset of light exposure (at t = 0) and zero at the time of complete dimerization. If we employ the plausible assumption that the ground-state monomer concentration is strictly decreasing with time during the exposure experiment, we can make the conservative estimation that at any final time T

$$\begin{aligned} N_{\mathrm{abs}}(T) &= I\frac{\lambda}{hc}\int_0^T \left(1 - e^{-\alpha \mathrm{M}(t)d}\right)dt \\ &> I\frac{\lambda}{hc}\int_0^T \left(1 - e^{-\alpha \mathrm{M}(T)d}\right)dt \\ &= IT\frac{\lambda}{hc}\left(1 - e^{-\alpha \mathrm{M}(T)d}\right) \end{aligned} \tag{4}$$

We can measure the function D(t) but not M(t). Nevertheless, at the time of half-dimerization ($T_{½}$) we know that the mass fraction of ground-state monomers is equal to, or slightly less than, the mass fraction of dimers, and we make the approximation that M($T_{½}$) ≈ ½. With this information at hand, we can calculate the lower limit for photons absorbed by ground-state monomers at $T_{½}$ as

$$\begin{aligned} N_{\mathrm{abs}}\left(T_{1/2}\right) &> IT_{1/2}\frac{\lambda}{hc}\left(1 - e^{-\left(\alpha \mathrm{M}\left(T_{1/2}\right)d\right)}\right) \\ &\approx IT_{1/2}\frac{\lambda}{hc}\left(1 - e^{-(\alpha d/2)}\right) \end{aligned} \tag{5}$$

By dividing Equation (1) with Equation (5), and correcting for that N_{dim} was calculated at full dimerization and N_{abs} at half dimerization, we get the following equation for the dimerization efficiency at half dimerization

$$\begin{aligned} \phi\left(IT_{1/2}\right) &= \frac{N_{\mathrm{dim}}/2}{N_{\mathrm{abs}}\left(T_{1/2}\right)} \\ &\approx \frac{\rho d N_{\mathrm{A}} hc}{4 M_{\mathrm{W}}\lambda\left(1 - e^{-(\alpha d/2)}\right)}\left(IT_{1/2}\right)^{-1} \end{aligned} \tag{6}$$

As Equation (6) only includes known and measured data, we can calculate the dependency of the dimerization efficiency φ on the factor $IT_{½}$, which is the exposure dose at half dimerization. This straightforward calculation reveals two interesting and important features. First, the dimerization efficiency is invariably very low. At the time $T_{½}$, φ is of the order of 10^{-3}. We can thus conclude that the assumption of negligible back-reaction paths must be wrong. Second, φ increases with increasing light intensity, as can be inferred from Equation (6) and the data presented in Figure 1c, where the latter reveals that the factor $IT_{½}$ decreases with increasing I. We will return to this second observation later on.

We now focus our attention on the issue of back reactions. As shown in Figure 2a, there are three possible back-reaction paths, governed by the k_2, k_4 and k_6 rate constants, which could rationalize the low value of φ. The high efficiency of the $^1M^* \rightarrow {}^3M^*$ intersystem crossing in fullerene systems, and the related consequence that the $^1M^* \rightarrow M$ back-transition is negligible, is well documented.[38,39] This fullerene-specific behavior is further manifested in a very low quantum yield for singlet exciton recombination, being ≈0.07% in C_{60}.[40] k_2 is consequently effectively equal to zero, and we accordingly cross out this back reaction in the simplified energy-level diagram presented in Figure 2b. Moreover, the consequence that an absorbed photon invariably results in the production of a $^3M^*$ state is conveniently indicated by the introduction of a parameter k_{13}, which governs the kinetics of the complete $M \rightarrow {}^3M^*$ transition. It is notable that the magnitude of k_{13} accordingly can be set effectively identical to k_1.

Further, we realize that a significant D → M dimer-dissociation back reaction, as quantified by the rate constant k_6, would be manifested in an incomplete dimerization of the film. Within the limits of accuracy of the experimental data presented in Figure 1c, we find that the film can be fully dimerized, and also

remain fully dimerized after a prolonged storage period in darkness. The rate constant k_6 is therefore set to zero. This conclusion is also in agreement with that the D → M dissociation has been demonstrated to be effectively zero below 400 K,[36,39,41] and that the utilized short exposure time and the significant thermal mass of the silicon wafer substrate (onto which the thin PCBM film is deposited) make it plausible that such an elevated temperature is never reached during our exposure experiments.

The only remaining possible back-reaction path is then the $^3M^* \rightarrow M$ relaxation, which is governed by the rate constant k_4. The well-established long lifetime of the $^3M^*$ state,[38] and a lack of information regarding the internal relationship between the rate constants k_4 and k_5, imply that this could be a viable back-reaction path. In consideration of that at least one significant back-reaction path must exist, and that the other possible back-reaction paths k_2 and k_6 are effectively zero, we select the $^3M^* \rightarrow M$ relaxation to be the significant back-reaction path in the simplified energy-level diagram in Figure 2b.

We now shift our attention to the final dimer-formation reaction. Eklund et al. concluded that the dimerization reaction takes place between a ground-state monomer and a neighboring triplet-excited monomer, i.e., $M + {}^3M^* \rightarrow D$, as quantified by the rate constant k_5 in Figure 2.[32,36] We term this mechanism the *uni-excited* molecular reaction. An alternative mechanism for the formation of dimers is the *bi-excited* molecular reaction, which is distinguished from the uni-excited molecular reaction in that *both* neighboring monomers need to be in the triplet-excited state for a dimerization to take place, i.e., $^3M^* + {}^3M^* \rightarrow D$. The bi-excited reaction is quantified by the rate constant k'_5 in Figure 2.

In order to evaluate the validity of the two different reaction models, we have performed a numerical-simulation study to establish whether any, or both, of the models are capable of reproducing the experimental data. We probed a wide range of discrete values for the rate constants k_{13}, k_4, k_5/k'_5, and allowed the numerical simulation to progress step-wise in time until complete dimerization was attained. Details on the numerical procedure, including the simulation code, are presented in the Supporting Information (section II).

We find that it indeed is possible to reproduce the experimental data with good accuracy by using the framework of the bi-excited model, and the attained excellent agreement between the experimental data and the bi-excited numerical-modeling data is clearly visible by comparing the graphs in **Figure 3**a,b. Furthermore, the value for the rate constant k_{13} is, as discussed earlier, effectively proportional to the light intensity *I*, and we call attention to that the ratios between the employed k_{13} values in Figure 3b are identical to the ratios between the different experimental *I* values in Figure 3a.

In contrast, we find that the uni-excited numerical modeling consistently fails in reproducing the experimental results (data not shown). More specifically, we find that the uni-excited modeling invariably results in a constant or decreasing value of the dimerization efficiency with increasing light intensity. With this observation in mind, we set out to analytically investigate whether the uni-excited model is compatible with the experimental observation that the dimerization efficiency increases with increasing light intensity *I* at constant exposure dose (below termed "*Dose*" for convenience). Considering that the rate constant k_{13} is effectively proportional to the light intensity, we can mathematically express this key experimental finding as

$$\left.\frac{d\,[\mathrm{D}]}{d\,I}\right|_{Dose} \propto \left.\frac{d\,[\mathrm{D}]}{d\mathrm{k}_{13}}\right|_{Dose} > 0. \tag{7}$$

The full set of rate equations for the uni-excited molecular reaction under the simplified scenario depicted in Figure 2b is

$$\frac{\partial\,[\mathrm{M}]}{\partial t} = -\mathrm{k}_{13}\,[\mathrm{M}] + \mathrm{k}_4\left[{}^3\mathrm{M}^*\right] - \mathrm{k}_5\left[{}^3\mathrm{M}^*\right][\mathrm{M}] \tag{8}$$

$$\frac{\partial\left[{}^3\mathrm{M}^*\right]}{\partial t} = \mathrm{k}_{13}\,[\mathrm{M}] - \mathrm{k}_4\left[{}^3\mathrm{M}^*\right] - \mathrm{k}_5\left[{}^3\mathrm{M}^*\right][\mathrm{M}] \tag{9}$$

$$\frac{\partial\,[\mathrm{D}]}{\partial t} = \mathrm{k}_5\left[{}^3\mathrm{M}^*\right][\mathrm{M}] \tag{10}$$

where the rate constants k_4 and k_5 are constants with respect to both time and light intensity, and k_{13} is held fixed. Mass conservation is considered by the equation

$$[\mathrm{M}] + \left[{}^3\mathrm{M}^*\right] + 2\,[\mathrm{D}] = [\mathrm{M}]_0\,, \tag{11}$$

where $[M]_0$ is a constant representing the initial concentration of monomers. Equation (11) implies that [D] at any final time *T* is completely defined by the variables [M] and $[^3M^*]$. Also, from Equation (10), the formation of dimers depends symmetrically on both [M] and $[^3M^*]$ in the uni-excited molecular reaction model, which is, to be noted, not the case in the bi-excited molecular reaction model. We can thus define [D] as a function of [M] and $[^3M^*]$, i.e. [D] = [D]([M], $[^3M^*]$). [M] and $[^3M^*]$

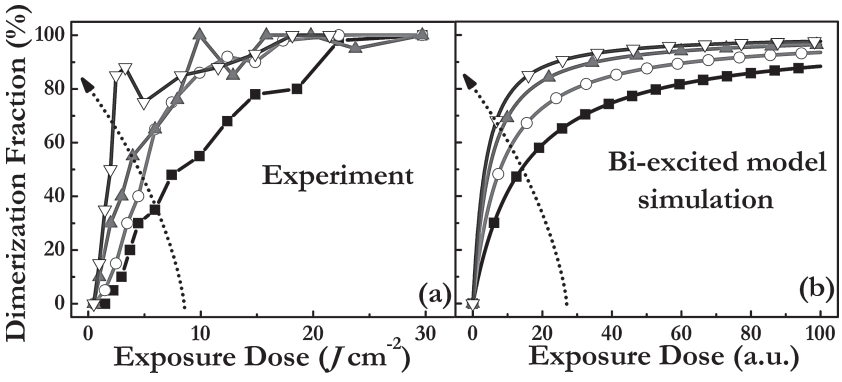

Figure 3. a) Experimental results: the curves represent exposure executed using different UV-light intensities, with the arrow indicating increasing intensity from 250 mW/cm^2 (solid squares), over 495 mW/cm^2 (open circles) and 990 mW/cm^2 (solid triangles), to 1650 mW/cm^2 (open triangles). b) Simulation results: the data are obtained employing a model comprising the simplified energy-level diagram (presented in Figure 2b) and a bi-excited molecular reaction. The exposure dose is given in arbitrary units, but the relative differences between the light intensities in the simulation are the same as in the experiments.

can in turn be defined as functions of time t and k_{13}. By taking the partial derivative of Equation (11) with respect to [M] and reordering we get

$$\frac{\partial [D]}{\partial [M]} = \frac{1}{2}\frac{\partial}{\partial [M]}\left([M]_0 - [M] - [^3M^*]\right) = -\frac{1}{2} \tag{12}$$

Similarly, by taking the partial derivative of Equation (11) with respect to $[^3M^*]$ we get

$$\frac{\partial [D]}{\partial [^3M^*]} = \frac{1}{2}\frac{\partial}{\partial [^3M^*]}\left([M]_0 - [M] - [^3M^*]\right) = -\frac{1}{2} \tag{13}$$

Now, with the time held constant, [M] and $[^3M^*]$ are only dependent on k_{13}. Applying the chain rule on the function [D] ([M], $[^3M^*]$), we have for fixed t that

$$\frac{\partial [D]}{\partial k_{13}} = \frac{\partial [D]}{\partial [M]}\cdot\frac{\partial [M]}{\partial k_{13}} + \frac{\partial [D]}{\partial [^3M^*]}\cdot\frac{\partial [^3M^*]}{\partial k_{13}} \tag{14}$$

Plugging in the results from Equations (12) and (13) into Equation (14), and reorganizing, we get

$$2\frac{\partial [D]}{\partial k_{13}} = -\frac{\partial [M]}{\partial k_{13}} - \frac{\partial [^3M^*]}{\partial k_{13}} \tag{15}$$

As the exposure light only acts to excite ground-state monomers to excited-state triplets (see Figure 2b) and is not involved in any other process, the *partial* derivative of [D] with respect to k_{13} is zero. Thus,

$$\frac{\partial [M]}{\partial k_{13}} = -\frac{\partial [^3M^*]}{\partial k_{13}} \tag{16}$$

Remembering that the light intensity I is proportional to k_{13}, and that I is kept constant during each measurement, we can express the exposure dose as

$$Dose = Dose\left(T\left(k_{13}\right), k_{13}\right) = \int_0^{T(k_{13})} \varepsilon k_{13} dt = \varepsilon k_{13} T, \tag{17}$$

where ε is a constant such that $\varepsilon k_{13} = I$. The condition of constant dose in Equation (7) means that we restrict the surface spanned by the final time T and k_{13} to a curve on which all points yield the same constant value for the *Dose*. On this curve we observe that

$$\left.\frac{dT}{dk_{13}}\right|_{Dose} = -\frac{Dose}{\varepsilon k_{13}^2} \tag{18}$$

Now, for constant *Dose*, we can state that

$$\begin{aligned}\left.\frac{d[D]}{dk_{13}}\right|_{Dose} &= \frac{\partial [D]}{\partial [M]}\cdot\frac{\partial [M]}{dk_{13}} + \frac{\partial [D]}{\partial [^3M^*]}\cdot\frac{\partial [^3M^*]}{\partial k_{13}} \\ &= \frac{\partial [D]}{\partial [M]}\cdot\frac{\partial [M]}{\partial T}\cdot\frac{dT}{dk_{13}} + \frac{\partial [D]}{\partial [M]}\cdot\frac{\partial [M]}{\partial k_{13}} \\ &+ \frac{\partial [D]}{\partial [^3M^*]}\cdot\frac{\partial [^3M^*]}{\partial T}\cdot\frac{dT}{dk_{13}} + \frac{\partial [D]}{\partial [^3M^*]}\cdot\frac{\partial [^3M^*]}{\partial k_{13}}.\end{aligned} \tag{19}$$

By using the results from Equations (12), (13) and (16), we find that the second and fourth term cancel. We are thus left with

$$\begin{aligned}\left.\frac{d[D]}{dk_{13}}\right|_{Dose} &= \frac{\partial [D]}{\partial [M]}\cdot\frac{\partial [M]}{\partial T}\cdot\frac{dT}{dk_{13}} + \frac{\partial [D]}{\partial [^3M^*]}\cdot\frac{\partial [^3M^*]}{\partial T}\cdot\frac{dT}{dk_{13}} \\ &= \frac{Dose}{2\varepsilon k_{13}^2}\left(\frac{\partial [M]}{\partial T} + \frac{\partial [^3M^*]}{\partial T}\right)\end{aligned} \tag{20}$$

where we have used Equations (12), (13) and (18) for the last simplification step. We know from the sum of Equations (8)–(10) that

$$\frac{\partial [M]}{\partial t} + \frac{\partial [^3M^*]}{\partial t} = -2\frac{\partial [D]}{\partial t} \tag{21}$$

for all t. Moreover, Equation (10) dictates that the time derivative of the concentration of dimers is positive for all non-zero t. Thus

$$\left.\frac{d[D]}{dk_{13}}\right|_{Dose} = -\frac{Dose}{\varepsilon k_{13}^2}\left(\frac{\partial [D]}{\partial T}\right) < 0 \tag{22}$$

and we can draw the conclusion that the uni-excited molecular reaction on analytical grounds is unable to account for our experimental findings.

3. Conclusions

We report experimental key findings related to the photochemical transformation of fullerene molecules, and develop a generic reaction model considering experimental data, analytical argumentation and numerical modeling. Specifically, we show that the efficiency of the photochemical monomer-to-dimer transformation of the commonly employed fullerene PCBM is strongly dependent on the light intensity, and that a patterning of an electronically active PCBM film can be effectuated by an ultrafast sub-second exposure of selective film areas to UV-light followed by development in a tuned acetone:chloroform solution. By analytical reasoning, we demonstrate that the observed intensity-dependent transformation dictates that a significant back-reaction to the ground state must be in effect, which presumably originates from the excited-triplet state. By modeling, we further show that the dimer formation must constitute a bi-excited reaction between two neighboring monomers photo-excited into the triplet state.

Supporting Information

Supporting Information is available from the Wiley Online Library or from the author.

Acknowledgements

This project was supported by Solar Fuels Umeå (Umeå University) and the Artificial Leaf Project Umeå (K&A Wallenberg foundation). The authors acknowledge the JC Kempe Foundation and the Swedish research council for research grants, and Professor Michael Bradley at Umeå University for stimulating discussions. L.E. is a "Royal Swedish

Academy of Sciences Research Fellow" supported by a grant from the Knut and Alice Wallenberg Foundation.

Received: November 19, 2012
Published online: January 23, 2013

[1] H. W. Kroto, J. R. Heath, S. C. Obrien, R. F. Curl, R. E. Smalley, *Nature* **1985**, *318*, 162.
[2] W. Kratschmer, L. D. Lamb, K. Fostiropoulos, D. R. Huffman, *Nature* **1990**, *347*, 354.
[3] L. Edman, A. Ferry, P. Jacobsson, *Macromolecules* **1999**, *32*, 4130.
[4] L. W. Barbour, M. Hegadorn, J. B. Asbury, *J. Am. Chem. Soc.* **2007**, *129*, 15884.
[5] L. Wang, B. B. Liu, D. Liu, M. G. Yao, Y. Y. Hou, S. D. Yu, T. Cui, D. M. Li, G. T. Zou, A. Iwasiewicz, B. Sundqvist, *Adv. Mater.* **2006**, *18*, 1883.
[6] T. Jovanovic, D. Koruga, B. Jovancicevic, V. Vajs, G. Devic, *Fullerines, Nanotubes, Carbon Nanostruct.* **2013**, *21*, 64.
[7] M. Feng, J. Zhao, H. Petek, *Science* **2008**, *320*, 359.
[8] R. C. Haddon, *Nature* **1995**, *378*, 249.
[9] I. V. Davydov, A. I. Podlivaev, L. A. Openov, *Phys. Solid State* **2005**, *47*, 778.
[10] J. Y. Kim, K. Lee, N. E. Coates, D. Moses, T. Q. Nguyen, M. Dante, A. J. Heeger, *Science* **2007**, *317*, 222.
[11] S. Watanabe, Y. Fukuchi, M. Fukasawa, T. Sassa, M. Uchiyama, T. Yamashita, M. Matsumoto, T. Aoyama, *Langmuir* **2012**, *28*, 10305.
[12] F. L. Wang, J. G. Tang, J. X. Liu, Y. Wang, R. Wang, L. Niu, L. J. Huang, Z. Huang, *Bull. Chem. Soc. Jpn.* **2011**, *84*, 427.
[13] R. D. Pensack, K. M. Banyas, L. W. Barbour, M. Hegadorn, J. B. Asbury, *Phys. Chem. Chem. Phys.* **2009**, *11*, 2575.
[14] N. Espinosa, H. F. Dam, D. M. Tanenbaum, J. W. Andreasen, M. Jorgensen, F. C. Krebs, *Materials* **2011**, *4*, 169.
[15] K. Maturova, R. A. J. Janssen, M. Kemerink, *ACS Nano* **2010**, *4*, 1385.
[16] Y. J. Cheng, C. H. Hsieh, P. J. Li, C. S. Hsu, *Adv. Funct. Mater.* **2011**, *21*, 1723.
[17] F. L. Zhang, K. G. Jespersen, C. Bjorstrom, M. Svensson, M. R. Andersson, V. Sundstrom, K. Magnusson, E. Moons, A. Yartsev, O. Inganas, *Adv. Funct. Mater.* **2006**, *16*, 667.
[18] Y. G. Wen, Y. Q. Liu, Y. L. Guo, G. Yu, W. P. Hu, *Chem. Rev.* **2011**, *111*, 3358.
[19] P. Strobel, J. Ristein, L. Ley, *J. Phys. Chem. C* **2010**, *114*, 4317.
[20] C. Waldauf, P. Schilinsky, M. Perisutti, J. Hauch, C. J. Brabec, *Adv. Mater.* **2003**, *15*, 2084.
[21] C. Larsen, J. Wang, L. Edman, *Thin Solid Films* **2012**, *520*, 3009.
[22] J. E. Anthony, A. Facchetti, M. Heeney, S. R. Marder, X. W. Zhan, *Adv. Mater.* **2010**, *22*, 3876.
[23] A. Dzwilewski, P. Matyba, L. Edman, *J. Phys. Chem. B* **2010**, *114*, 135.
[24] T. D. Anthopoulos, D. M. de Leeuw, E. Cantatore, S. Setayesh, E. J. Meijer, C. Tanase, J. C. Hummelen, P. W. M. Blom, *Appl. Phys. Lett.* **2004**, *85*, 4205.
[25] P. Zhou, Z. H. Dong, A. M. Rao, P. C. Eklund, *Chem. Phys. Lett.* **1993**, *211*, 337.
[26] A. F. Hebard, C. B. Eom, R. M. Fleming, Y. J. Chabal, A. J. Muller, S. H. Glarum, G. J. Pietsch, R. C. Haddon, A. M. Mujsce, M. A. Paczkowski, G. P. Kochanski, *Appl. Phys. A: Mater. Sci. Process.* **1993**, *57*, 299.
[27] S. McGinnis, L. Norin, U. Jansson, J. O. Carlsson, *Appl. Phys. Lett.* **1997**, *70*, 586.
[28] A. Dzwilewski, T. Wågberg, L. Edman, *Phys. Rev. B* **2007**, *75*, 075203.
[29] A. Dzwilewski, T. Wågberg, L. Edman, *J. Am. Chem. Soc.* **2009**, *131*, 4006.
[30] J. Wang, C. Larsen, T. Wågberg, L. Edman, *Adv. Funct. Mater.* **2011**, *21*, 3723.
[31] A. M. Rao, P. Zhou, K. A. Wang, G. T. Hager, J. M. Holden, Y. Wang, W. T. Lee, X. X. Bi, P. C. Eklund, D. S. Cornett, M. A. Duncan, I. J. Amster, *Science* **1993**, *259*, 955.
[32] Y. Wang, J. M. Holden, Z.-H. Dong, X.-X. Bi, P. C. Eklund, *Chem. Phys. Lett.* **1993**, *211*, 341.
[33] S. L. Ren, Y. Wang, A. M. Rao, E. McRae, J. M. Holden, T. Hager, K. Wang, W.-T. Lee, H. F. Ni, J. Selegue, P. C. Eklund, *Appl. Phys. Lett.* **1991**, *59*, 2678.
[34] Y. Wang, J. M. Holden, A. M. Rao, W.-T. Lee, X. X. Bi, S. L. Ren, G. W. Lehman, G. T. Hager, P. C. Eklund, *Phys. Rev. B* **1992**, *45*, 14396.
[35] J. B. Birks, *Photophysics of aromatic molecules*, Wiley-Interscience, London **1970**.
[36] P. C. Eklund, A. M. Rao, P. Zhou, Y. Wang, J. M. Holden, *Thin Solid Films* **1995**, *257*, 185.
[37] C. W. T. Bulle-Lieuwma, W. J. H. van Gennip, J. K. J. van Duren, P. Jonkheijm, R. A. J. Janssen, J. W. Niemantsverdriet, *Appl. Surf. Sci.* **2003**, *203–204*, 547.
[38] J. W. Arbogast, A. P. Darmanyan, C. S. Foote, F. N. Diederich, R. L. Whetten, Y. Rubin, M. M. Alvarez, S. J. Anz, *J. Phys. Chem.* **1991**, *95*, 11.
[39] Y. Wang, J. M. Holden, X.-x. Bi, P. C. Eklund, *Chem. Phys. Lett.* **1994**, *217*, 413.
[40] P. A. Lane, L. S. Swanson, Q. X. Ni, J. Shinar, J. P. Engel, T. J. Barton, L. Jones, *Phys. Rev. Lett.* **1992**, *68*, 887.
[41] M. Sakai, M. Ichida, A. Nakamura, *Fullerene Sci.Technol.* **2001**, *9*, 351.